Mineral. Soc. Amer. Spec. Pap. **3,** 85–93 (1970).

PETROLOGY OF THE MANTLE[1]

DON L. ANDERSON
Seismological Laboratory, California Institute of Technology, Pasadena, California

ABSTRACT

Recent seismic results indicate a series of transition regions or "discontinuities" in the mantle. These can be interpreted in terms of phase changes in olivine, pyroxene, and garnet. The low-velocity zone is due to partial melting, and it may also be enriched in heavy elements relative to adjacent regions of the mantle. Free oscillation interpretations indicate that the upper mantle has a density of at least 3.5 gm/cm³. Seismic data for the lower mantle combined with shock wave data suggest that the lower mantle is richer in FeO than previously supposed. The lower mantle is closer to pyroxene in composition than to olivine.

INTRODUCTION

Recent developments in several different fields have set the stage for a discussion of the composition and crystal structure of the various regions of the mantle. These developments include (1) increasingly detailed seismic velocity profiles for the mantle, (2) the emergence of density as an independently determinable property of the mantle, (3) the availability of shock wave data on rocks and minerals at pressures and temperatures relevant to the deep mantle, (4) an ever increasing inventory of ultrasonic measurements on rocks and minerals, including the effects of temperature and pressure, and (5) experimental petrological measurements up to about 200 kbars which have determined the stability fields and crystal structure of high-pressure mantle minerals and analog compounds. The above data are augmented by X-ray static compression measurements, heat flow measurements, seismic attenuation studies and laboratory studies on presumed upper mantle rocks including their melting behavior.

RECENT SEISMIC RESULTS—BODY WAVES

Surface waves, free oscillations, large seismic arrays and large underground explosions, have been used by seismologists to considerably refine the standard velocity-depth profiles of Bullen, Gutenberg, Jeffreys, and Lehmann. The most important result concerns the critical but controversial transition region, Bullen's Region C, between about 400 and 1000 km depth. Surface-wave studies (Anderson and Toksoz, 1963) showed that this region was not a broad 600-km thick zone of transition but was made up of a series of relatively thin (~50 km) regions of very rapid increase in velocity. The most notable of these "discontinuities" occur at depths near 400 and 600 km. These results have been verified by a large number of surface wave and body wave studies, and can be explained in detail by a series of solid-solid phase changes in a predominately olivine mantle (Anderson, 1967a).

Figure 1 shows several recent upper mantle models. In addition to the "discontinuities" or transition regions, the upper mantle low-velocity zone is a persistent feature of most recent studies although the details vary from region to region. This part of the mantle also attenuates seismic waves very rapidly (Anderson and Archambeau, 1964, Anderson *et al.* 1965, Anderson, 1967C).

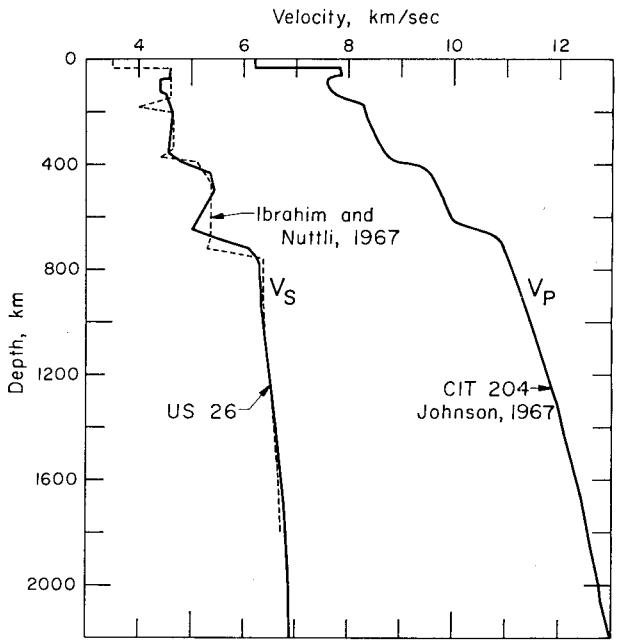

FIG. 1. Recent shear wave and compressional wave profiles for the upper mantle after Johnson (1967), Ibrahim and Nuttli (1967), and Anderson and Julian (1969).

Evidence for other, much smaller, discontinuities in the mantle has also been found. Reflecting horizons have been found at 50, 130, 280, 410, 520, 630, 940, and 1250 km (Whitcomb and Anderson, in preparation). Other small discontinuities have been found at 830, 1000, 1230, 1540, and 1910 km (Archambeau *et al.*, 1969; Johnson, 1969).

Most of the discontinuities can be attributed to solid-solid phase changes which have been directly observed in the laboratory or inferred from studies of the behavior of analog compounds, shock wave studies or crystal chemical considerations. Above some 400 km normal upper mantle minerals such as olivine, pyroxene, and garnet are stable in their low pressure phases. Near 400 km olivine collapses to the spinel or β-spinel phase with a 7 to 10 percent increase in density but no change in the coordination of silicon. At somewhat higher pressure pyroxene is unstable. These intermediate pressure phases have a limited stability

[1] Contribution No. 1708, Division of Geological Sciences, California Institute of Technology.

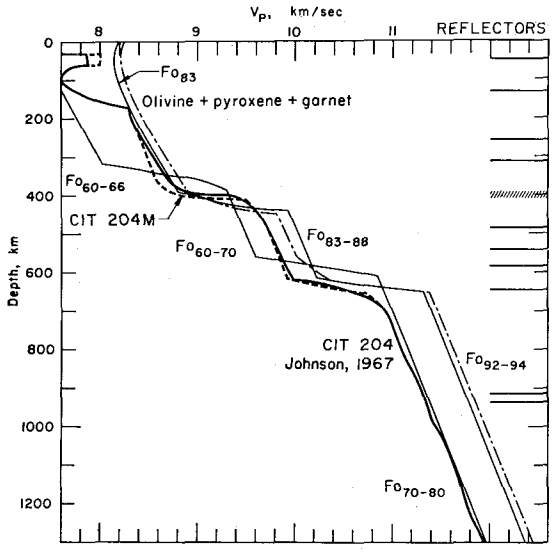

FIG. 2. Two recent compressional velocity profiles for the upper mantle compared with velocities to be expected in olivine and peridotite mantles (modified from Anderson, 1966). Olivine is assumed to undergo successive phase changes, first to the spinel structure and then to a structure with silicon in six-fold coordination. Pyroxene is assumed to disproportionate to spinel+stishovite and then to transform to the silicon six-fold coordination. Garnet is assumed to remain stable throughout the region shown. The smaller discontinuities below 600 km may represent a garnet transformation. Reflectors, shown to the right, are derived from a study of precursors to the double core phase P'P' (Whitcomb and Anderson, in prep.).

field, as shown by shock wave and thermochemical studies, and transform to still denser assemblages which probably involve an increase in the coordination of silicon.

There is some evidence, to be discussed later, that the mantle is not uniform in composition and this raises the possibility that some of the discontinuities in the mantle are due to compositional changes.

Discontinuities as Phase Changes

The major phases of the upper mantle are probably olivine, pyroxene, and garnet. All of these structures are unstable at high pressure and go through a series of polymorphic transitions. Olivine is the most studied upper mantle mineral and is also probably the most abundant. There is remarkable quantitative agreement between the seismic data and that predicted for a pure olivine mantle. The agreement includes the absolute value of the seismic velocity gradient, the depth and magnitude of the "discontinuities" and the thickness of the transition regions. Figure 2 shows the compressional velocity profiles of Johnson (1967) and Julian and Anderson (1968). The depths of reflecting horizons (Whitcomb and Anderson, in preparation) are shown to the right and indicate, in addition to the boundaries of the low-velocity zone and the two major transition regions, that "discontinuities" occur near 280, 520, 940, and 1250 (not shown) km depth. The two light solid curves are velocities to be expected in a pure olivine mantle with composition as indicated undergoing a series of breakdowns, first to the spinel structure and then to a hypothetical structure having the density and thermodynamic properties of a mixture of MgO, SiO_2 (stishovite), and FeO. The density versus depth was computed using finite strain theory and a pressure dependent coefficient of thermal expansion. The compressional velocity was estimated from the density by using a modification of Birch's velocity-density relationship (Birch, 1961b). The range in composition associated with each curve indicates our ignorance of the effect of iron on the elastic properties. Note that the "theoretical" velocity decreases with depth until about 50 km. This is due to the large temperature gradient in the upper mantle which more than cancels out the effect of pressure. This is a phenomenon that occurs for nearly any reasonable geotherm and choice of material. Velocities which decrease with depth are to be expected in homogeneous regions of the crust and upper mantle. However the upper mantle low-velocity zone is much too pronounced to be the effect of a high temperature gradient; this will be discussed in the next section.

The dash-dot curve in Figure 2 shows the estimated compressional velocity profile for a more realistic mantle which is composed of pyroxene and garnet as well as olivine. The pyroxene phase is assumed to disproportionate to spinel plus stishovite and then to the oxides. This introduces a region of high velocity gradient starting slightly below 500 km and provides a possible explanation for the reflection observed at 520 km. A feature similar to that calculated was inferred by Helmberger (personal communication) from a study of compressional wave amplitudes. It apparently is too subtle a feature to be picked up in conventional studies of travel times and apparent velocities. Garnet is assumed to remain stable throughout the region shown.

The stability fields for forsterite and fayalite are shown in Figures 3 and 4. Once the equilibrium line is established

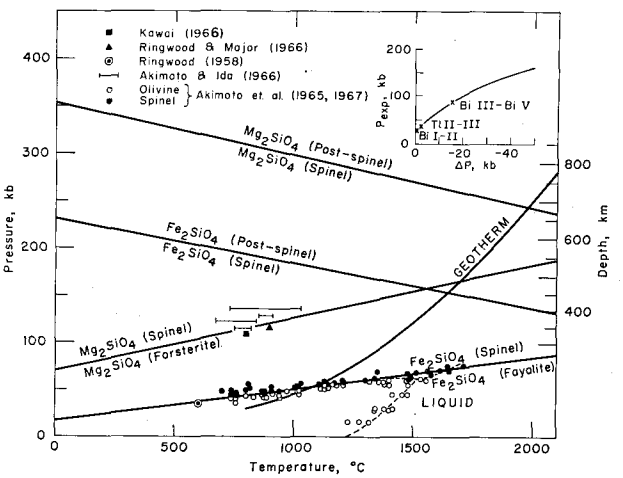

FIG. 3. Stability fields of forsterite and fayalite and a representative geotherm.

for the olivine-spinel phase change the spinel to post-spinel equilibrium boundary can be computed (Anderson, 1967a). Both phase changes involve about a 10 percent increase in density which, except for the end members, will be spread out over some tens of kilometers. The depths and detail of the transition regions in Figure 2 are computed from these phase diagrams.

It has recently been found (Ringwood and Major, 1970) that the olivine-spinel phase diagram is not as simple as that shown in Figure 4. An additional phase, β-spinel, has been found to intervene between the stability fields of olivine and spinel near the forsterite rich end. The β-spinel phase is about $7\frac{1}{2}$ percent denser than the olivine phase. A schematic phase diagram, along the geotherm, is shown in Figure 5 which is adapted from Ringwood's isothermal phase diagram. The insert shows schematically the resulting velocity depth relation. The phase diagram, as drawn, offers an alternate explanation for the transition near 500 km.

Any phase changes between 200 and 400 km must be much smaller than those at 400 and 600 km since they have not been observed with conventional body wave refraction techniques. They involve either a smaller density (velocity) jump in a major component or involve a component much less abundant than olivine. Ringwood and Major (1966b) found that at high pressure garnet will dissolve pyroxene with a consequent increase in density. This will proceed at 350-400 km for an iron free system and probably at shallower depths in the presence of Fe^{2+}. Ferromagnetic phase changes may also be important in this region for minerals containing iron ions.

The deeper discontinuities are also relatively small. Possibilities include the collapse of pyroxene and garnet to an ilmenite or related structure and a disproportionation of garnet to the oxides MgO, FeO, Al_2O_3 and SiO_2 (stishovite). If the lower mantle is a mechanical mixture of the simple oxides, the collapse of (Mg, Fe)O rocksalt structure to the cesium chloride structure and a transformation of SiO_2 to

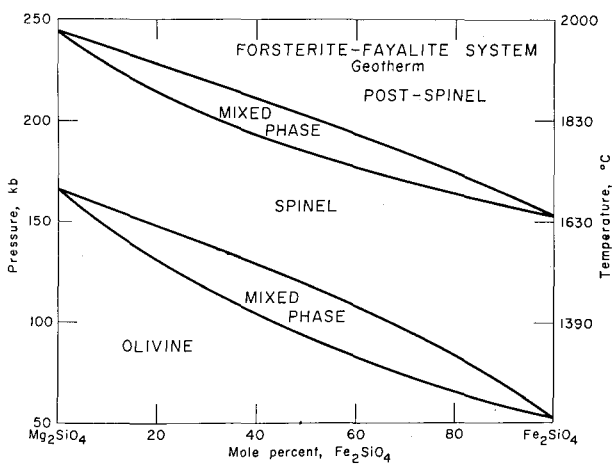

FIG. 4. Phase diagram of $Mg_2SiO_4-Fe_2SiO_4$ system assuming ideal solid solution.

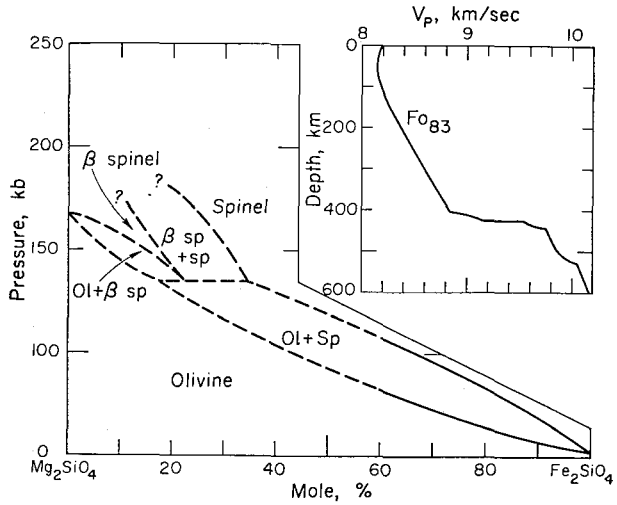

FIG. 5. Phase diagram for olivine system modified from Ringwood (1969). Insert shows expected compressional velocity profile for a forsterite rich olivine mantle. See also Akimoto (1969).

the PbF_2 structure must be considered, but shock wave data argues against these happening at mantle pressures. Minerals containing Fe^{2+} can be expected to undergo a spin-spin transition (high spin to low spin) at about 1400 km. This transition discussed by Strens (1969) involves a large decrease in the ionic radius of Fe^{2+} and, for typical mantle compounds, would involve a density change of several percent. This phase change would tend to stabilize iron in the lower mantle and, because of ionic radii considerations, would probably reverse the usual tendency for the iron-rich end member of an isostructural series to have a lower melting point than the magnesium rich end member. The first melt in this region of the mantle would probably be magnesium rich.

The Low-Velocity Zone

The low-velocity zone is often considered to be the result of high thermal gradients in this region of the mantle. The effect of temperature and pressure on the elastic velocities of a variety of oxides and silicates have been tabulated by Anderson *et al.* (1968). Using these data and recent velocity profiles it can be inferred that temperature gradients of 19-24°C/km between about 50 and 100 km are required to produce the compressional velocity decrease (Anderson and Sammis, 1969). The corresponding gradient required to produce the shear velocity decrease is 9-13°C/km. Inferred heat flow through the top of the mantle would be 1.1 to 1.4 μm cal/cm^2 sec in the former case and 0.5 to 0.8 μm cal/cm^2 sec in the latter. These gradients and heat flow values are inconsistent with each other and the former is inconsistent with heat flow interpretations. In addition, such gradients would intercept melting point curves of postulated mantle rocks at 100 km or less.

The drop in velocity in the low-velocity zone amounts to about 3 percent. Spetzler and Anderson (1968) measured

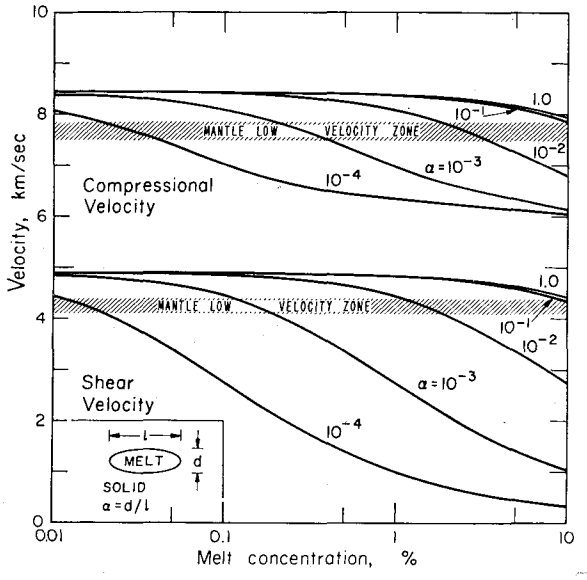

FIG. 6. Compressional and shear velocity as a function of melt concentration and aspect ratio, α, for an olivine containing basaltic melt. Curves are based on the theory of Walsh (1969) and the parameters of Birch (1969).

the change in velocity across the eutectic temperature in the $NaCl \cdot H_2O$ system. They found that a small amount of melt considerably decreased the velocity and increased the attenuation of ultrasonic waves. The results depended on the shape of the melt zones as well as the total melt content but extrapolation of their results indicate that about 1 percent melt could cause a 3 percent change in velocity. This is a much greater effect than one would predict with a simple model of spherical melt zones embedded in a solid matrix. Birch (1969) used such a model and derived a molten fraction of about 6 percent to explain the reduction of velocity in the low-velocity zone.

Walsh (1969) developed a theory for the effect of elliptical melt zones on the velocities of elastic waves. Input parameters are the compressional and shear velocity of the matrix, the compressional velocity and volume fraction of the melt and the aspect ratio of the molten zones. Using the room temperature properties of olivine for the matrix and of basalt glass for the melt (Birch, 1969) we obtained the curves in Figure 6. The upper curves are for spherical melt zones ($\alpha = 1.0$) and are taken from Birch's paper. If we used 1200°C velocity values, more appropriate for the upper mantle, the compressional velocity curves would be lowered by about 0.68 km/sec and the shear velocity curves would be lowered by about 0.39 km/sec. For comparison the velocities in the low-velocity zone are shown stippled. If melting is confined to grain boundaries we would expect relatively small aspect ratios.

For example, using the high temperature velocities an aspect ratio of 10^{-2} would satisfy the seismic data with 1 percent melt. The effect on density would be negligible.

If partial melting occurs in the upper mantle the temperature gradient would probably approximate the melting point gradient which is 10°C/km for most dry rocks and slightly less for rocks containing small amounts of water. This is much lower than gradients required to produce the compressional wave low-velocity zone in the absence of melting. As discussed by Anderson and Sammis (1969) partial melting in the upper mantle probably requires the presence of a small amount of water.

Partial melting is an attractive explanation for the low-velocity zone since it explains the abrupt boundaries, the total decrease in velocity, and the increased seismic attenuation. The low-velocity zone may also differ in composition from the adjacent mantle.

RECENT SEISMIC RESULTS—FREE OSCILLATIONS

The study of free oscillations of the Earth complements classical body wave seismology in that the free oscillations are sensitive to density as well as the velocities of compressional and shear waves. Free oscillations are particularly sensitive to the density in the upper mantle and this is important in discussing the possible composition of this region. For example Figure 7 shows the effect on the period of one of the spheroidal modes of the various parameters. Note the importance of density in the upper mantle. Other modes show similar behavior.

Figure 8 shows some recent Earth models which satisfy the periods of free oscillation, the mass and moment of the Earth and travel times of body waves. All models have a relatively high density in the upper 100 km or so of the mantle, 3.5 to 3.6 b/cm$_3$. This is significantly higher than the conventional value of about 3.3 g/cm^3. Press (1969) reached a similar conclusion.

In order to satisfy the seismic data a peridotite upper

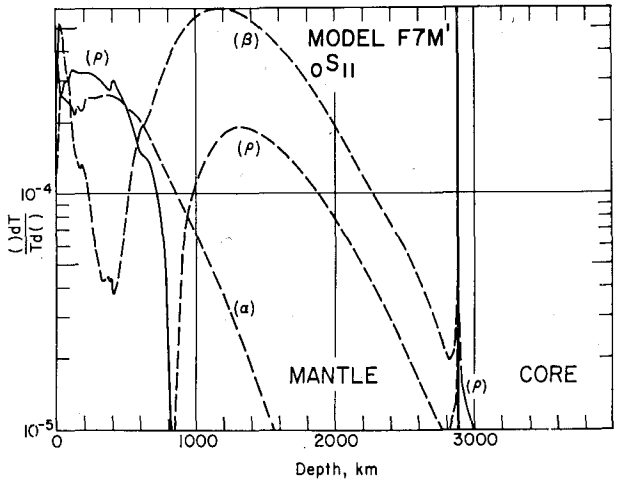

FIG. 7. Free oscillation variational parameters for spheroidal mode $_0S_{11}$ showing the importance of density, ρ, in the upper mantle. For this mode the most important parameter is shear velocity β, in the middle mantle and this is determined from body wave studies. Most of the modes of free oscillation are not very sensitive to the compressional velocity, α.

mantle must contain substantial amounts of FeO and/or TiO_2. This would require that most rocks of presumed upper mantle orgin are not representative of the total composition, but represent the low-density, *high* melting point fraction. Basalts would represent the low-density, low-melting point fraction of the upper mantle and the low-velocity zone would be rich in the low-melting point high-density iron, and possibly titanium-rich silicates. The upper mantle, down to the bottom of the low-velocity zone, in this view, can be considered to be gravitationally stratified.

An alternate point of view is that the upper mantle is composed of eclogite. Some eclogites have the required velocities and density. The basaltic oceanic crust is generally considered to be derived by fractional melting, up to 30 percent, from the underlying mantle. Since eclogite is the high pressure chemical equivalent of basalt, total melting would be required, at least locally, to generate basalt magma from the upper mantle.

The values for density, compressional velocity and shear velocity at 200 km corrected to 10 kb and room temperature can be compared with the ultrasonic results of Birch (1961a) at the same conditions. All three properties are less than found by Birch for the Twin Sister's dunite. Reasonable agreement can be obtained by mixing the dunite with peridotite, bronzitite or eclogite. The inferred mineralogy is 45 to 75 percent olivine, 25 to 50 percent pyroxene, and up to about 15 percent garnet.

Composition of the Lower Mantle

Unfortunately, the most precise seismic data for the lower mantle, namely the compressional and shear velocities, cannot be compared directly with laboratory data. Shock wave experiments, however, allow a direct comparison of the density after an approximate allowance has been made for the effect of temperature. Figure 9 shows density versus pressure for two dunites of different iron content. The raw Hugoniot data are shown along with low-temperature adiabats and adiabats that are appropriate for mantle temperatures. The density curve for the lower mantle, derived from free oscillation data is also shown. In the oversimplified case of a pure olivine (in the post-spinel phase) lower mantle the implied fayalite content is 18–19 percent, much greater than usually assumed.

Another property of the lower mantle can be inferred from the seismic velocities. The seismic parameter Φ, defined as

$$\Phi = V_p^2 - (4/3)V_s^2 = (V_s^2 = (\partial P/\partial \rho)_s = K_s/\rho$$

where V_p and V_s are the two seismic velocities, ρ is the density, P the pressure and K_s is the adiabatic bulk modulus or incompressibility. This parameter can be obtained experimentally by taking the slope of the adiabat which is derived from shock wave studies, a parameter closely related to the hydrodynamic sound velocity.

Anderson (1967b) using elastic constant data for oxides and silicates, developed an empirical relationship between

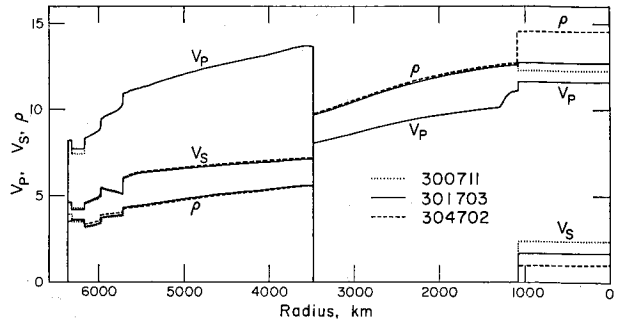

FIG. 8. Earth models resulting from the inversion of free oscillation data (Anderson and Smith, 1968).

the zero pressure values of density and the seismic parameter Φ which involved the parameter $\overline{M}$, the mean atomic weight. He also discussed the effect of temperature and pressure on this relationship which is called the seismic equation of state. Anderson and Kanamori (1968) and Ahrens *et al* (1969) utilized this relationship to infer the zero pressure density of the high pressure phases induced in shock experiments. There is a systematic tendency for Φ to increase with density and to decrease with mean atomic weight. The zero-pressure properties, ρ_0 and $\Phi_0 = (\partial P/\partial \rho)_0$, of shock induced phases can be estimated by fitting an equation of state to the shock wave data with the constraint that the above properties satisfy the seismic equation of state at zero pressure. Results for some rocks and minerals are given in Table 1 where a modified form of the Φ–ρ relationship, appropriate for close-packed structures, has been used (Anderson, 1969).

A similar procedure can be used to extrapolate lower mantle seismic data to zero pressure conditions (Anderson and Jordan, 1969). Using free oscillation models, the results are $\rho_0 = 4.40$ g/cm^3 and $\Phi_0 = 61.3$ (km/sec)^2, slightly higher than conventional earth models in which the mass and moment of inertia of the earth are the main constraints on density. For example, Birch Model 2 (Birch, 1961b) gives $\rho_0 = 4.16$ g/cm^3 and $\Phi_0 = 59.6$ (km/sec)^2. Looking at Table 1 we see that the density can be matched by an iron rich olivine or dunite, but the mantle Φ_0 cannot. Interpolating between Fo_{90}, Fo_{45}, and stishovite we can satisfy both ρ_0 and Φ_0 with 18 mole percent FeO, 32 mole percent MgO, and 50 mole percent SiO_2. This is the stoichiometry for an iron rich pyroxene, *i.e.* $(Mg_{0.64}\ Fe_{0.36})SiO_3$. Taken at face value this would indicate that the lower mantle is enriched in SiO_2 relative to the upper mantle. The issue is complicated by some shock wave data on pure forsterite which give high values for ρ_0 and Φ_0 (Anderson and Kanamori, 1968, Ahrens *et al* 1969) but the forsterite data is not as extensive as that shown in Figure 9 for the dunites. More shock wave data is needed for forsterite and for pyroxene rich rocks.

Anderson (1969) showed that the Φ for complex oxides was approximately equal to the molar average of the Φ of the component oxides. By averaging the values of Φ for

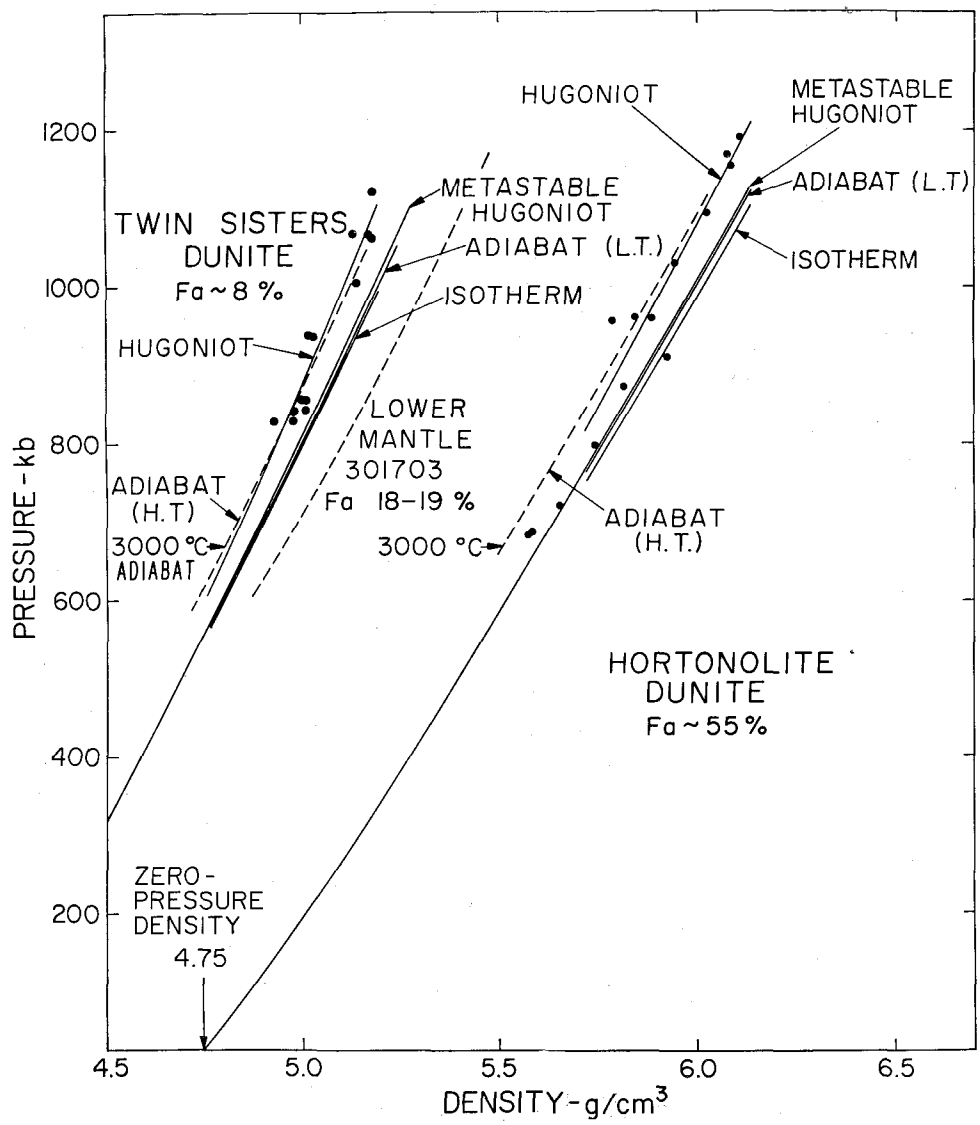

FIG. 9. Shock wave data for two dunites obtained by McQueen *et al.* (1967). Low temperature adiabats and isotherms calculated by Ahrens *et al.* (1969). Lower mantle curve from free oscillation studies (Anderson and Smith, 1968.)

MgO, FeO, Al_2O_3 and SiO_2 (stishovite) we can estimate the zero pressure properties of the high pressure phases of olivine, pyroxene, and garnet as shown in Figure 10. Also shown are two mantle models which bracket published solutions for the lower mantle. Model 200204 is a free oscillation model of Anderson and Smith (1968). The inferred lower mantle composition is given in Table 2. In terms of weight percent, Birch 2 gives 45, 38, and 17 percent, respectively, for SiO_2, MgO, and FeO. These can be compared with conventional estimates of the composition of the upper mantle which give 50, 41, and 9 percent for these components. The free oscillation model gives 51, 28, and 21 percent for SiO_2, MgO, and FeO, respectively, in weight percent which represents an enrichment of FeO in the lower mantle in agreement with the conclusion reached above.

The crystallography of the lower mantle is a subject that has received scattered attention since Thompson and Birch (Birch, 1952) predicted a high-pressure rutile form for SiO_2. Experimental petrologists have not yet reached lower mantle pressures and their standard quenching techniques, to recover and examine phases which are metastable at

TABLE 1. COMPOSITION OF LOWER MANTLE (IN MOLE FRACTION)

Model	Olivine	Pyroxene	Garnet	SiO_2	MgO	FeO
Birch 2	0.57	0.43	—	0.39	0.49	0.12
Birch 2	0.50	—	0.50	—	—	—
200204	0.20	0.80	—	0.46	0.38	0.16
200204	0.10	—	0.90	—	—	—

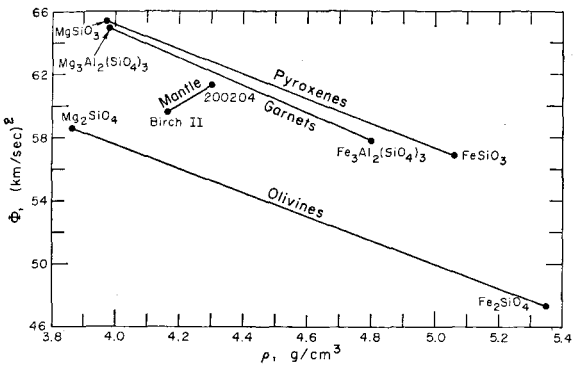

FIG. 10. Density, ρ, vs. seismic parameter Φ for high pressure phases of olivine, garnet and pyroxene based on the hypothesis of additivity of Φ (Anderson, 1969). Two mantle models are also shown. Free oscillation results imply a lower mantle richer in FeO and SiO_2 than conventional mantle models.

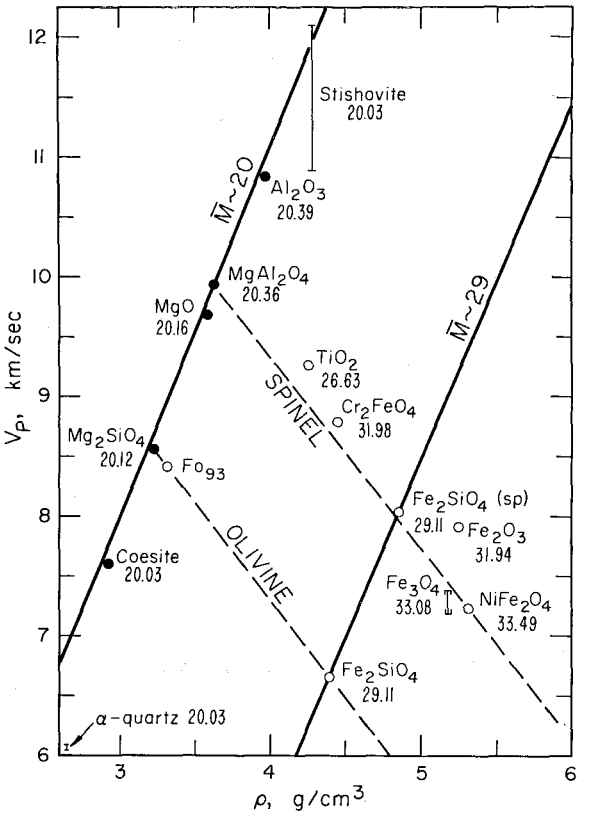

FIG. 11. Compressional velocity vs. density for oxides and silicates. Data from Anderson *et al.* (1968), Mitzutani *et al.* (1970) and Lieberman (pers. commun.)

room conditions, would probably not be adequate. Shock wave recovery experiments are just now being attempted, although stishovite has been recovered from both meteorite impacts and laboratory experiments.

Speculations regarding the crystal structure of high-pressure silicate phases are based primarily on structures and phase changes of analog isoelectronic compounds, especially those having larger cation radii than Mg, Fe, Al, and Si. This technique has been exploited with great success by Ringwood (*e.g.* Ringwood, 1970). High-pressure shock wave data gives some indication of possible high pressure structures in silicates and oxides. Table 1 gives results which are based on the method developed by Anderson and Kanamori (1968) using the modified seismic equation of state (Anderson, 1969) to relate ρ and $\partial P/\partial\rho$ at $P=0$. Crystal structures which may be important at high pressure include calcium ferrite, potassium nickel fluoride, strontium plumbate, perovkite, ilmenite, rocksalt and rutile (see also Ahrens *et al.*, 1969). Although the densities of silicates in these phases can be estimated, ultrasonic measurements are required on more of these structures before it is clear how closely they can satisfy the other seismic data. In any event, it is quite probable that the

TABLE 2. INFERRED ZERO-PRESSURE DENSITY AND Φ_0 OF HIGH-PRESSURE SHOCK-INDUCED PHASES: $\rho_0=0.0492\,\overline{M}\,\Phi^{1/3}$

Substance	Formula	Φ_0 (km/sec)²	ρ_0 (g/cm³)	Isochemical mixed oxides ρ (g/cm³)	Other possible structures	Structure density ρ (g/cm³)
Spinel	$MgAl_2O_4$	65.5	4.03	3.86	$CaFe_2O_4$	4.13
Magnetite	$FeFe_2O_4$	52.9	6.11	5.54	Fe_3O_4 (LS)	5.62
					$CaFe_2O_4$	5.84
					$HPFe_2O_3$+Fe	6.1
					FeO+Fe_2O_3 (perovskite)	5.94
Hematite	Fe_2O_3	47.7	5.70		Fe_2O_3 (LS)	5.94
					perovskite	5.8
Olivine	$Fo_{90}Fa_{10}$	53.9	3.94	4.04	Ca_2SnO_4	4.04
					K_2MgF_4	4.3
Olivine	$Fo_{45}Fa_{55}$	51.3	4.59	4.64	Ca_2SnO_4	4.64
Fayalite	Fe_2SiO_4	43.3	5.03	5.29	Ca_2SnO_4	5.29
					Spinel	4.85
					Spinel (LS)	5.61
					Olivine (LS)	5.18
Stishovite	SiO_2	70	4.29			

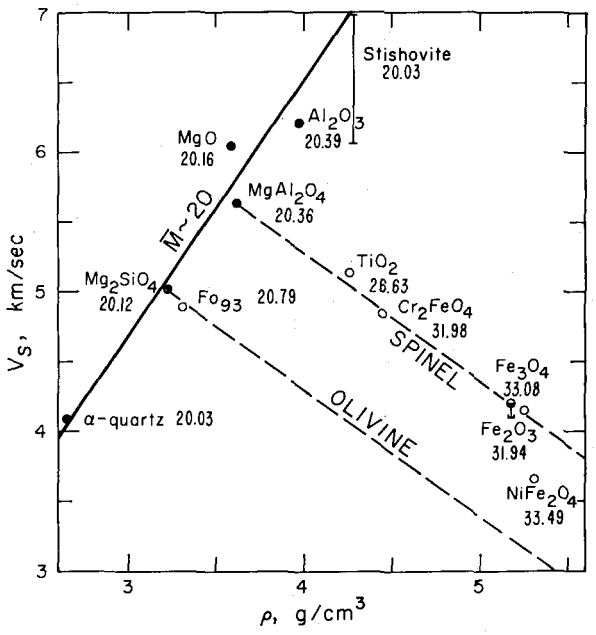

FIG. 12. Shear velocity vs. density for oxides and silicates.

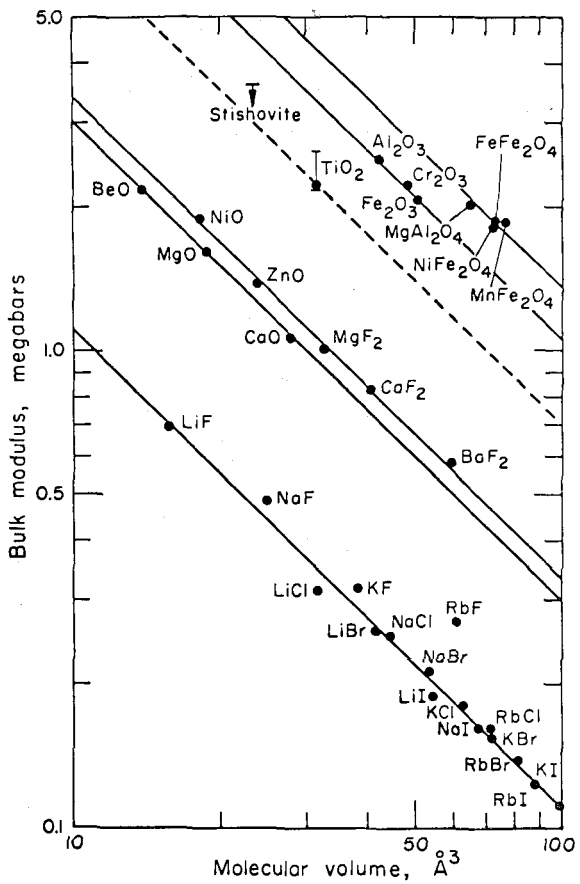

FIG. 13. Bulk modulus vs. molecular volume for halides and oxides after Anderson and Anderson (1970).

lower mantle is composed of phases which involve silicon in six-fold coordination, as in stishovite.

VELOCITY-DENSITY SYSTEMATICS

Ultrasonic measurements of the elastic properties of rocks and minerals provide the basic data for interpreting seismic results in terms of composition, particularly of the upper mantle. Measurements on analog compounds, not necessarily of mantle composition, of various crystal structures are important in estimating the velocity in high pressure phases which are inaccessible for direct measurement. Birch (1961b) proposed a linear relationship between density and compressional velocity for rocks using ultrasonic data from his laboratory. He proposed several density models for the mantle using this relation. Now that density can be determined independently, velocity-density systematics will be useful in determining the composition throughout the mantle.

Birch (1961b) introduced the parameter $\overline{M}$, mean atomic weight and showed that density and compressional velocity were linearly related for rocks and minerals having the same mean atomic weight. Figure 11 illustrates this point and shows, further, that minerals having the same crystal structure also line up. Note that coesite, forsterite, periclase corundum and spinel, all having a mean atomic weight of about 20, fall near the same line, even though they all have quite different crystal structures. The situation is not so simple for shear velocity, Figure 12, but trends are still evident. As one might expect the shear velocity is not as simple a function of mean atomic weight and density, but it also depends on the crystal structure.

The systematics for bulk modulus versus molecular volume are evident in Figure 13. In this case, the theory is better developed. For example, using ionic solid theory with an exponential repulsive parameter we can write

$$K = \frac{Az_1z_2e^2(r/\rho - 2)}{Vr}$$

where K, A, V, r, Z are the bulk modulus, Madelung constant, molecular volume, interatomic distance, and valence, respectively. The repulsive range parameter is ρ. The structure of the crystal enters via the Madelung constant.

Using these figures it should be possible to estimate the velocities corresponding to various proposed crystal structures for the various regions of the mantle.

ACKNOWLEDGMENTS

The author benefitted from discussions with E. Gaffney and A. E. Ringwood. G. Davies kindly recalculated the densities of the high pressure shock phases given in Table 1. M. Smith, T. Jordan, and F. Klein were involved in various aspects of the research reported in this paper. This research was supported by National Science Foundation Grant GA 12703.

References

AHRENS, T. J., DON L. ANDERSON, AND A. E. RINGWOOD (1969) Equations of state and crystal structures of high-pressure phases of shocked silicates and oxides. *Rev. Geophys.*, **7**, 667–708.

AKIMOTO, S., (1969) High-pressure transformations in $(MgFe)_2SiO_4$ olivine, $(MgFe)SiO_3$ pyroxene and other silicates. (abstr) *Int. Sym. Phase Transform. Earth Interior, Canberra.*

AKIMOTO, S., AND Y. IDA (1966) High pressure synthesis of Mg_2SiO, spinel, *Earth Planet. Sci. Lett.*, **1**, 358–359.

———, H. FUJISAWA, AND T. KATSURA (1965) The olivine-spinel transition in Fe_2SiO_4 and Ni_2SiO_4. *J. Geophys. Res.*, **70**, 1969–1977.

———, E. KOMADA, AND I. KUSHIRO (1967) Effect of pressure on the melting of olivine and spinel polymorphs of Fe_2SiO_4. *J. Geophys. Res.*, **72**, 679–686.

ANDERSON, DON L. (1966) The earth's viscosity. *Science*, **151**, 321–322, 1966.

———, (1967a) Phase changes in the mantle, *Science*, **157**, 1165–1173.

———, (1967c) The anelasticity of the mantle, *Geophys. J.*, **14**, 135–164.

———, (1969) Bulk modulus-density systematics, *J. Geophys. Res.* **74**, 3857–3864.

———, AND ORSON L. ANDERSON (1970) Bulk modulus-density relations, *J. Geophys. Res.*, in press,

———, AND C. ARCHAMBEAU (1964) The anelasticity of the earth, *J. Geophys. Res.*, **69**, 2071–2084.

———, AND T. JORDAN (1969) The composition of the lower mantle, *Phys. Earth Planet. Interiors*, in press.

———, AND B. JULIAN (1969) Shear velocities and elastic parameters of the mantle, *J. Geophys. Res.*, **74**, 3281–3286.

———, AND H. KANAMORI (1968) Shock wave-equations of state for rocks and minerals, *J. Geophys. Res.*, **73**, 6477–6502.

———, AND C. SAMMIS (1969) Partial melting in the mantle. *Phys. Earth Planet. Interiors, in press.*

———, AND M. SMITH (1968) Mathematical and physical inversion of gross earth data (abstr.) *Trans. Amer. Geophys. Union*, **49**, 282.

———, AND M. N. TOKSOZ (1963) Surface waves on a spherical earth. I. Upper mantle structure from Love Waves. *J. Geophys. Res.*, **68**, 3483–3500.

———, A. BEN-MENAHEM, AND C. ARCHAMBEAU (1965) Attenuation of seismic energy in the upper mantle. *J. Geophys. Res.*, **70**, 1441–1448,

ANDERSON, O. L., E. SCHREIBER, R. C. LIEBERMANN, AND N. SOGA (1968) Some elastic constant data on minerals relevant to geophysics. *Rev. Geophys.*, **6**, 491–524.

ARCHAMBEAU, C. B., E. A. FLINN, AND D. G. LAMBERT (1969) Fine structure of the upper mantle, *J. Geophys. Res.*, **74**, 5825–5866.

BIRCH, F. (1952) Elasticity and constitution of the earth's interior, *J. Geophys. Res.*, **57**, 227–286.

———, (1961a) The velocity of compressional waves in rocks to 10 kilobars, 2. *J. Geophys. Res.* **66**, 2199–2224.

———, (1961b) Composition of the earth's mantle. *Geophys. J.*, **4**, 205–311.

———, (1969) Density and composition of the upper mantle: First approximation as an olivine layer *Amer. Geophys. Union Geophys. Mon.* **13**, 18–36.

IBRAHIM, A. K., AND O. NUTTLI (1967) Travel-time curves and upper mantle structure from long-period S waves. *Bull. Seis. Soc. Amer*, **57**, 1063–1092.

JOHNSON, L. (1967) Array measurements of P velocities in the upper mantle, *J. Geophys. Res.* **72**, 6309–6325.

———, (1969) Array measurements of P velocities in the lower mantle, *Bull. Seis. Soc. Amer*, **59**, 973–1008.

JULIAN, B., AND DON L. ANDERSON (1968) Travel times, apparent velocities and amplitudes of body waves. *Bull. Seis. Soc. Amer.* **58**, (1) 339–366.

KAWAI, N., S. ENDOH, AND S. SAKATA (1966) Synthesis of Mg_2SiO_4 with a spinel structure. *Proc. Jap. Acad.* **42**, 626–628.

MCQUEEN, R. G., S. P. MARSH, AND J. N. FRITZ (1967) Hugoniot equation of state of twelve rocks. *J. Geophys. Res.* **72**, 4999–5036.

MITZUTANI, H., Y. HAMANO, Y. IDA, AND S. AKIMOTO (1970) Compressional wave velocities of fayalite, Fe_2SiO_4 spinel, and coesite, *J. Geophys. Res.*, in press.

PRESS, F. (1969) The suboceanic mantle. *Science*, **165**, 174–176.

RINGWOOD, A. E. (1958) Constitution of the Mantle, II. Further data on the olivine spinel transition. *Geochim. Cosmochim. Acta*, **15**, 18–29.

———, (1970) Phase transformations and the constitution of the mantle, *Phys. Earth Planet, Interiors.* in press.

———, AND A. MAJOR, (1966a) Synthesis of Mg_2SiO_4-Fe_2SiO_4 solid solutions, *Earth Planet. Sci. Lett.* **1**, 241–245.

———, AND ——— (1966b) High pressure transformations in pyroxenes, *Earth Planet. Sci. Lett.* **1**, 351–357.

———, AND ——— (1970) The system Mg_2SiO_4—Fe_2SiO_4 at high pressures and temperatures. *Phys. Earth Planet. Interiors.* in press.

SPETZLER, H., AND DON L. ANDERSON (1968) The effect of temperature and partial melting on velocity and attenuation in a simple binary system. *J. Geophys. Res.*, **73**, 6051–6060.

STRENS, R. G. J. (1969) The nature and geophysical importance of spin pairing in minerals of iron, II. *In The Application of Modern Physics to the Earth and Planetary Interiors*, Wiley-Interscience, New York.

WALSH, J. B. (1969) New analysis of attenuation in partially melted rock, *J. Geophys. Res.* **74**, 4333–4337.